ANALYTICAL PARAMETRIC CYCLE ANALYSIS OF CONTINUOUS ROTATING DETONATION EJECTOR-AUGMENTED ROCKET ENGINE

by

HUAN V. CAO

Presented to the Faculty of the Graduate School of
The University of Texas at Arlington in Partial Fulfillment
of the Requirements
for the Degree of

MASTER OF SCIENCE IN AEROSPACE ENGINEERING

THE UNIVERSITY OF TEXAS AT ARLINGTON
May 2011

ACKNOWLEDGEMENTS

I would like to thank Dr. Donald Wilson for showing me how interesting the topic of continuous detonation is for the application of high speed propulsion. The manner in which he taught graduate propulsion courses, especially hypersonic propulsion, inspired me to further enjoy researching into this topic as a promising concept for propulsion. He was fairly helpful whenever I have questions popping out of my head and would make himself available in person for thorough discussions on certain aspects of this thesis project.

I would also like to thank Eric Braun for providing some insights and advice on the physics of continuous detonation. His dedication and enthusiasm for his related field of study brings out a sense of admiration from me for this kind of work.

Finally, I would like to owe my debt of appreciation to my brother and my parents for inspiring me to keep up the determination on pursuing higher education in my field of interest no matter how rough it may be.

April 18, 2011

ABSTRACT

ANALYTICAL PARAMETRIC CYCLE ANALYSIS OF

CONTINUOUS ROTATING DETONATION

EJECTOR-AUGMENTED

ROCKET ENGINE

Huan Cao, M.S.

The University of Texas at Arlington, 2011

Supervising Professor: Dr. Donald Wilson

An analytical parametric cycle analysis model for the continuous rotating detonation wave ejector-augmented rocket was developed to estimate and evaluate the maximum potential performance that the continuous rotating detonation wave rocket (CRDWR) itself can provide in an ejector ramjet as well as the two-stage rocket for low earth orbit (LEO). This was done by integrating Bykovskii's model for CRDWR with Heiser & Pratt's modified ejector ramjet and their transatmospheric performance model. The performance results of this unique engine in comparison to a regular rocket counterpart were evaluated primarily in terms of specific thrust and specific impulse with respect to flight Mach number in a constant dynamic pressure trajectory as well as in terms of initial payload mass ratio for a transatmospheric trajectory to LEO.

TABLE OF CONTENTS

LIST OF ILLUSTRATIONS

LIST OF TABLES

CHAPTER 1

INTRODUCTION

For years, various attempts were made to improve the performance of air-breathing and rocket engines. One improvement was undertaken by revolutionizing the way fuels are burned, which is by using detonation waves. For decades, traditional burning of fuel like deflagration has been used in engines in which the flame front travels at low subsonic speed through the fuel-oxidizer mixture. But detonation itself can combust the mixture more efficiently than deflagration and in many cases burn the mixture more intensely. While deflagration produces mostly heat, detonation in combustion produces both heat and high pressure almost simultaneously, both of which is needed to produce high specific thrust in an engine. It is known that pressure in the rocket combustion chamber needs to be very high to produce high thrust with high specific impulse. With detonation, the established pressure in the chamber can be lower since the detonation wave will increase the pressure significantly as it passes through the fuel-oxidizer mixture. Under identical initial conditions in the chamber, combustion through detonation produces a lower entropy rise as compared to deflagration [1].

1.1 Bykovskii's Continuous Detonation Model

There are various types of detonation wave engine concepts. One of them is continuous detonation wave engine where the detonation process continues as long as the propellant reactants are fed into the chamber while the combustion products are removed from the chamber [1]. A specific concept of this category is the continuous rotating (spin) detonation wave in an annular cylindrical chamber proposed by Voitsekhovskii where combustion of the mixture is achieved by a transverse detonation wave (TDW) moving perpendicularly to the main axial direction of the mixture and reaction products [1]. The TDW travels in a circumferential

trajectory in the chamber while the propellant mixture is renewed behind each passing TDW front as shown in Figure 1.1 below [1].

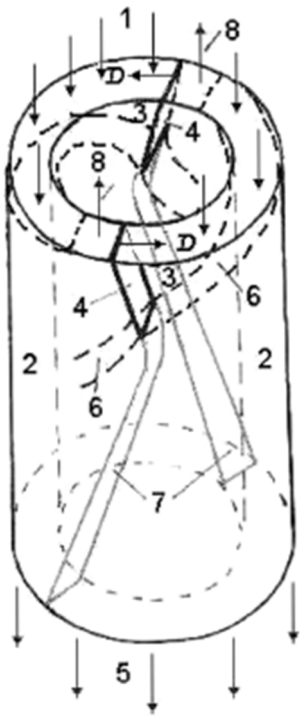

Figure 1.1 Diagram of TDW in annular cylindrical chamber [Ref 1].

In Figure 1.1, the TDW, represented by number 4, is traveling counter-clockwise with an adjacent trailing oblique shock wave represented by number 7 [1]. A fresh propellant mixture is formed before each TDW as represented by number 3 [1]. The TDW then propagates through region 3 to combust that mixture [1]. Compared to the pulsed detonation engine (PDE), this does not require a complete purging of the combustion products from the entire chamber nor filling the entire chamber with the propellant mixture before each detonation process. While the PDE operates in a frequency of tens of hertz, the continuous rotating detonation wave engine can operate in a range of thousands of hertz, making the operation a more steady-state process than that of a PDE. To help gain a better understanding of this concept, the focus of this study

will be aimed particularly at the rocket propulsion model of this concept, which was developed extensively by Bykovskii and others at the Institute of Hydrodynamics (LIH) [1].

1.2 Project Objective

The purpose of this project study was to develop an analytical parametric cycle analysis model to estimate the maximum potential performance that the continuous rotating detonation wave rocket (CRDWR) can provide in an ejector ramjet as well as a two-stage rocket for low earth orbit (LEO). This was done by integrating Bykovskii's rocket model for continuous rotating detonation with Heiser & Pratt's ejector ramjet and their transatmospheric performance model [2]. The propellants used for such cases were diatomic hydrogen and oxygen for fuel and oxidizer since they are commonly used in today's rockets. For a basic level of performance comparison with a regular H_2-O_2 rocket, the initial pressure and temperature of the chamber of the continuous rotating detonation wave rocket were 1 atm and 300 K before combustion, which are essentially sea-level atmospheric conditions. This was done to keep the focus more on the effect of performance due to the different combustion mechanisms of these two engines rather than the high total pressures in their rocket chambers.

CHAPTER 2

ANALYTICAL METHODOLOGY FOR PERFORMANCE ANALYSIS

The first thing to do is to develop a parametric cycle analysis on Bykovskii's CRDWR model based on his theoretical equations [1]. The exhaust exit parameters from that analysis is then fed as inputs into Heiser & Pratt's ejector ramjet model to calculate the engine performance for a constant dynamic pressure, q_O, trajectory from takeoff to hypersonic speeds. Those parameters are also put into Heiser & Pratt's two-stage transatmospheric model to calculate engine performance in terms of initial payload mass ratio for LEO.

2.1 Parametric Cycle Analysis of Bykovskii's CRDWR

The aim is to put together a parametric cycle analysis to calculate the gas properties from the exhaust exit of the annular chamber of the CRDWR, utilizing Bykovskii's theoretical equations for his CRDWR model. This analysis in particular does not include any nozzle since the goal is to calculate total gas properties specifically, such as total temperature, T_t, and total pressure, P_t, as well as gamma, γ, and the gas constant, R, which are input parameters for the ejector ramjet cycle analysis. Another parametric cycle analysis will be built upon this analysis later on where a nozzle is added to this model for a two-stage launch vehicle.

With that in mind, the first step is to select a fuel and oxidizer and their corresponding pressure and temperature before combustion. In this case, it is diatomic hydrogen and oxygen with both having a pressure of 1 atm and a temperature of 300 K in the annular rocket chamber. Axially, they both have a certain injection velocity, but in a transverse direction with respect to the rotating detonation wave, the initial velocity is approximately zero. With that information, the gas properties across the detonation wave is then calculated using NASA's CEA code [3]. The

information that is extracted from that program is the molecular weight of the combusted gas behind the detonation wave, γ_{det}, its temperature, T_{det}, and its speed of sound, a_{det}. From that, the gas constant behind the detonation wave is calculated by this relation shown below [4]:

$$R_{\text{det}} = \frac{\widetilde{R}}{M_{\text{det}}} \tag{1}$$

where $\widetilde{R}$ is the universal gas constant and M_{det} is the molecular weight of the combusted gas [4]. The specific heat at constant pressure of the combusted gas, $c_{P,\text{det}}$, is then determined by this relation (4):

$$c_{P,\text{det}} = \frac{\gamma_{\text{det}} R_{\text{det}}}{\gamma_{\text{det}} - 1} \tag{2}$$

With $c_{P,\text{det}}$, the total enthalpy of the combusted gas behind the wave can be calculated by this relation:

$$h_O = c_{P,\text{det}} T_{\text{det}} + \frac{V_{\text{det}}{}^2}{2} \tag{3}$$

where the absolute total velocity behind the wave, V_{det}, which includes the velocity components in both the axial and transverse direction, is equal to a_{det} according to the Bykovskii model [1]. While the absolute transverse component of this velocity is equal to the TDW's Chapman-Jouguet (CJ) velocity minus the sonic velocity behind the wave, the axial component of this velocity is due to the new propellant mixture that is pushing the old combustion products forward in the annular chamber for the next coming detonation wave.

Now the next thing is to select a value for input parameters for the parametric cycle analysis such as the outer diameter of the annular chamber, d_C, the ratio of fresh combustible mixture layer height to the distance between succeeding transverse detonation waves, $\frac{h_1}{l}$, and

the number of transverse detonation waves, n [1]. For simplicity for this analytical analysis, it shall be assumed that no fraction of combustion products will pass through another TDW from the preceding TDW. Therefore, the value of k, which is the fraction of the total mass flux from the preceding TDW that passes through the next TDW, is zero and the height of the fresh mixture layer in front of each TDW, h_1, is equal to the height of the TDW, h, as shown in this relation [1]:

$$h_1 = (1-k)h \tag{4}$$

Since the aim is to determine the maximum potential performance that the CRDWR is capable of, the relationship between the optimal length of the annular cylindrical chamber, L_{opt}, and h was used to calculate $\frac{h_1}{l}$ for the best continuous detonation process for the CRDWR as shown below [1]:

$$L_{opt} \geq 4h \cong 0.7l \tag{5}$$

In this case, $h_1 = h$, which would equate to $\frac{h_1}{l} = 0.175$. The distance between the TDW's is then calculated with this relation [1]:

$$l = \frac{\pi d_C}{n} \tag{6}$$

which is then used to calculate h_1 directly with this relation [1]:

$$h_1 = \frac{h_1}{l} l \tag{7}$$

With that, the distance between the annular walls, Δ, for a chamber of possible minimum size is determined by this relation [1]:

$$\Delta \geq \Delta^* \cong 0.2h \tag{8}$$

The propellant flow rate across each TDW, G_1, is then calculated with this relation [1]:

$$G_1 = h_1 \Delta \rho_2 q_2 \tag{9}$$

where ρ_2 is the density of the combusted gas behind the TDW and q_2 is the total velocity of that gas, which is equal to the speed of sound behind the TDW, c_2, according to Bykovskii [1]. The specific flow rate of the propellant in the axial direction, g, is then determined by this relation [1]:

$$g = \frac{G_1}{\Delta l} \tag{10}$$

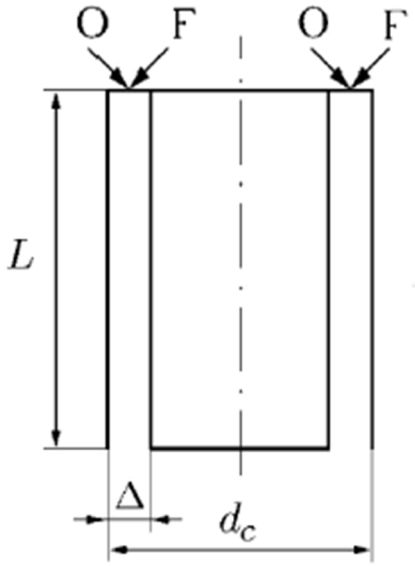

Figure 2.1 Schematic diagram of combustion annular chamber [1].

From that point, the exit parameters for the constant annular cylindrical chamber configuration of the CRDWR as shown in Figure 2.1 above, can finally be calculated, which are exit velocity, V_e, exit pressure, P_e, and exit density, ρ_e. They are determined by these relations below [1]:

$$V_e = \sqrt{\frac{2(\gamma_{\text{det}} - 1)h_O}{(\gamma_{\text{det}} + 1)}} \tag{11}$$

$$P_e = \frac{gV_e}{\gamma_{\det}} \tag{12}$$

$$\rho_e = \frac{g}{V_e} \tag{13}$$

With those parameters, the specific impulse, I_{sp}, of the CRDWR can finally be calculated, which is the maximum value for an annular chamber at vacuum ambient pressure with no nozzle. The I_{sp} is determined with the assumption that the axial exit velocity of the chamber is the sonic velocity and is found by this relation [1]:

$$I_{sp} = \frac{P_e + \rho_e V_e^2}{g} = \frac{\sqrt{2(\gamma_{\det}{}^2 - 1)h_O}}{\gamma_{\det}} \tag{14}$$

2.2 Parametric Cycle Analysis of Ejector CRDWR

Based on the exit parameters of the CRDWR, the next step is to determine the input parameters of the primary flow for the ejector ramjet where the CRDWR acts as the primary core engine. The aim is to calculate the performance of the ejector ramjet in a constant dynamic pressure, q_O, trajectory with the CRDWR utilized. This is done by using the parametric cycle analysis of Heiser & Pratt's ideal ejector ramjet model as illustrated in Figure 2.2 below [2].

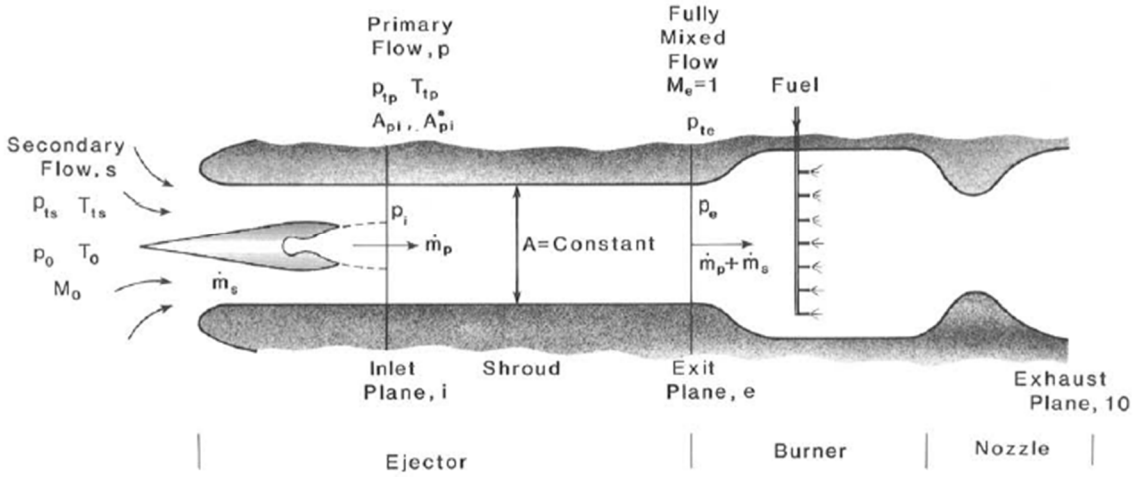

Figure 2.2 Schematic diagram of ejector ramjet [2].

The input parameters of the primary flow for the ejector ramjet are the ratio of total exit pressure of the CRDWR to ambient pressure, $\frac{P_{tp}}{P_O}$, ratio of total exit temperature of the CRDWR to ambient temperature, $\frac{T_{tp}}{T_O}$, γ_p, and the gas constant of the primary flow, R_p. To calculate these parameters, the speed of sound at the exit, a_e, the static exit temperature, T_e, and the exit Mach number, M_e, from the exhaust of the CRDWR engine in the primary flow must first be determined, which are found by these relations below:

$$a_e = \sqrt{\gamma_{\text{det}} \frac{P_e}{\rho_e}} \tag{15}$$

$$M_e = \frac{V_e}{a_e} \tag{16}$$

$$T_e = \frac{a_e^{\,2}}{\gamma_{\text{det}} R_{\text{det}}} \tag{17}$$

From there, the total temperature and total pressure from the primary engine can finally be calculated by these relations:

$$T_{te} = T_e \left(1 + \frac{\gamma_{\text{det}} - 1}{2} M_e^{\,2} \right) \tag{18}$$

$$P_{te} = P_e \left(1 + \frac{\gamma_{\text{det}} - 1}{2} M_e^{\,2} \right)^{\frac{\gamma_{\text{det}}}{\gamma_{\text{det}} - 1}} \tag{19}$$

They are then divided by the ambient parameters to get $\frac{T_{tp}}{T_O}$ and $\frac{P_{tp}}{P_O}$ as shown below:

$$\frac{T_{tp}}{T_O} = \frac{T_{te}}{T_{amb}} \tag{20}$$

$$\frac{P_{tp}}{P_O} = \frac{P_{te}}{P_{amb}} \tag{21}$$

The ambient pressure and temperature would correspond to flight conditions along the constant q_O trajectory. The dynamic pressure itself can be a function of flight Mach number and ambient pressure as shown below [2]:

$$q_O = \frac{1}{2}\gamma_O P_O M_O^{\,2} \tag{22}$$

The ambient pressure, P_O, in that above equation would correspond to a certain altitude, from which the value of ambient temperature can be determined. The gas constant and gamma value (specific heat ratio) of the primary flow are the exit parameters from the CRDWR as shown in these relations below:

$$R_p = R_{\text{det}} \tag{23}$$

$$\gamma_p = \gamma_{\text{det}} \tag{24}$$

The reason behind those relations is because the exhaust flow of the CRDWR is the expansion of combustion products from behind the TDW [1]. Therefore, the exhaust gas only consists of combustion products from behind each TDW.

For the input parameters of the secondary flow of the ejector ramjet, they are M_O, $\frac{P_{ts}}{P_O}$, $\frac{T_{ts}}{T_O}$, γ_s, and R_s. The flight Mach number, M_O, is set as an input control variable for the constant q_O trajectory, which for this study is q_O equal to 47,880 N/m^2 (1000 lbf/ft^2). The total pressure ratio, the total temperature ratio, γ_s, and the gas constant of the secondary flow can be determined by these relations below [5]:

$$\gamma_s = \gamma_{air} \tag{25}$$

$$\frac{P_{ts}}{P_O} = \pi_d \frac{P_{tO}}{P_O} \tag{26}$$

$$\frac{T_{ts}}{T_O} = 1 + \frac{\gamma_s - 1}{2} M_O{}^2 \tag{27}$$

$$R_s = R_{air} \tag{28}$$

where $\frac{P_{tO}}{P_O} = \left(1 + \frac{\gamma_s - 1}{2} M_O{}^2\right)^{\frac{\gamma_s}{\gamma_s - 1}}$ and $\pi_d = \pi_{d,\max} \eta_r$ [5]. In this study, the value of $\pi_{d,\max}$ is 0.96 using level 4 technology for supersonic aircraft with the engine in the airframe [5]. The total pressure recovery of the supersonic inlet, η_r, is estimated by this relation below for military specification MIL-E-5008B [5]:

$$\eta_r = \begin{cases} 1 & M_O \le 1 \\ 1 - 0.075\left(M_O - 1\right)^{1.35} & 1 < M_O < 5 \\ \dfrac{800}{M_O{}^4 + 935} & 5 < M_O \end{cases} \tag{29}$$

With the input parameters determined, the parametric cycle analysis of the ejector ramjet can be carried out by first calculating the Mach number of the primary and secondary flow right before they start mixing in the shroud, which are determined by these relations below [2, 6]:

$$M_{pi} = \sqrt{\frac{2}{\gamma_p - 1}\left(\left[\frac{P_{tp}/P_O}{P_i/P_O}\right]^{\frac{\gamma_p - 1}{\gamma_p}} - 1\right)} \tag{30}$$

$$M_{si} = \sqrt{\frac{2}{\gamma_s - 1}\left(\left[\frac{P_{ts}/P_O}{P_i/P_O}\right]^{\frac{\gamma_s - 1}{\gamma_s}} - 1\right)} \tag{31}$$

where $\frac{P_i}{P_O}$ is the static pressure ratio used as an iteration parameter for the parametric cycle analysis of the ejector ramjet [2]. The ratio of area of the primary flow before mixing over the throat area of the primary flow, $\frac{A_{pi}}{A_p^*}$, the ratio of area of the primary flow before mixing over the shroud area of the ejector ramjet, $\frac{A_{pi}}{A}$, and the ratio of area of the secondary flow before mixing over the shroud area, $\frac{A_{si}}{A}$, are then calculated in the following order [2, 6]:

$$\frac{A_{pi}}{A_p^*} = \frac{1}{M_{pi}}\left[\frac{2}{\gamma_p+1}\left(1+\frac{\gamma_p-1}{2}M_{pi}^{\ 2}\right)\right]^{\frac{\gamma_p+1}{2(\gamma_p-1)}} \tag{32}$$

$$\frac{A_{pi}}{A} = \frac{A_{pi}/A_p^*}{A/A_p^*} \tag{33}$$

$$\frac{A_{si}}{A} = 1-\frac{A_{pi}}{A} \tag{34}$$

where $\frac{A}{A_p^*}$ is the input parameter for the cross-sectional size of the ejector ramjet [2]. The bypass ratio of the ejector ramjet, α, which is the ratio of the secondary mass flow rate to the primary mass flow rate is given by this relation [2, 6]:

$$\alpha = \frac{P_{ts}/P_O}{P_{tp}/P_O}\left(\frac{A_{si}/A}{A_{pi}/A}\right)\frac{M_{si}}{M_{pi}}\sqrt{\frac{T_{tp}/T_O}{T_{ts}/T_O}\left(\frac{\gamma_s R_p}{\gamma_p R_s}\right)}\frac{\left(1+\frac{\gamma_p-1}{2}M_{pi}^{\ 2}\right)^{\frac{\gamma_p+1}{2(\gamma_p-1)}}}{\left(1+\frac{\gamma_s-1}{2}M_{si}^{\ 2}\right)^{\frac{\gamma_s+1}{2(\gamma_s-1)}}} \tag{35}$$

The specific heat at constant pressure for the primary, secondary, and fully mixed flow are then determined by these relations below [2, 6]:

$$C_{pp} = \frac{\gamma_p R_p}{\gamma_p - 1} \tag{36}$$

$$C_{ps} = \frac{\gamma_s R_s}{\gamma_s - 1} \tag{37}$$

$$C_{pe} = \frac{C_{pp} + \alpha C_{ps}}{1 + \alpha} \tag{38}$$

Note that the fully mixed flow is at station *e* of the ejector ramjet, which is the reason for the subscript notation at this point of the parametric cycle analysis. With that, the gas constant and γ_e of the fully mixed flow in the ejector ramjet can be calculated by these relations below [2, 6]:

$$R_e = \frac{R_p + \alpha R_s}{1 + \alpha} \tag{39}$$

$$\gamma_e = \frac{C_{pe}}{C_{pe} - R_e} \tag{40}$$

Afterwards, the ratio of total temperature of the fully mixed flow over ambient temperature, $\frac{T_{te}}{T_O}$, and the ratio of its total pressure over ambient pressure, $\frac{P_{te}}{P_O}$, can then be determined by these relations below [2, 6]:

$$\frac{T_{te}}{T_O} = \frac{1}{1+\alpha}\frac{C_{pp}}{C_{pe}}\frac{T_{tp}}{T_O} + \frac{\alpha}{1+\alpha}\frac{C_{ps}}{C_{pe}}\frac{T_{ts}}{T_O} \tag{41}$$

$$\frac{P_{te}}{P_O} = \frac{\frac{P_{tp}}{P_O}\frac{A_{pi}}{A} M_{pi} \sqrt{\frac{R_e}{R_p}\left(\frac{T_{te}/T_O}{T_{tp}/T_O}\right)\frac{\gamma_p}{\gamma_e}\left(\frac{1+\gamma_e}{2}\right)^{\frac{\gamma_e+1}{2(\gamma_e-1)}}}(1+\alpha)}{\left(1+\frac{\gamma_p-1}{2}M_{pi}^{\,2}\right)^{\frac{\gamma_p+1}{2(\gamma_p-1)}}} \tag{42}$$

The ratio of static pressure of the fully mixed flow over ambient pressure, $\frac{P_e}{P_O}$, can be calculated by this relation [2, 6]:

$$\frac{P_e}{P_O} = \frac{P_e}{P_{te}} \frac{P_{te}}{P_O} \tag{43}$$

where $\frac{P_e}{P_{te}} = \left(\frac{2}{\gamma_e + 1} \right)^{\frac{\gamma_e}{\gamma_e - 1}}$ for a fully mixed flow at sonic Mach number. The total pressure and static pressure of that flow can be individually found by these relations below:

$$P_{te} = \frac{P_{te}}{P_O} P_O \tag{44}$$

$$P_e = \frac{P_e}{P_O} P_O \tag{45}$$

The solution for the parametric cycle analysis of the ejector ramjet converges when the iterated value of $\frac{P_i}{P_O}$ is such that the following relation below based on the conservation of mass and momentum is satisfied [2, 6].

$$\frac{\frac{P_e}{P_O}\left(1 + \gamma_e\right)}{\frac{P_i}{P_O}\left[\frac{A_{pi}}{A}\left(1 + \gamma_p M_{pi}^{\ 2}\right) + \frac{A_{si}}{A}\left(1 + \gamma_s M_{si}^{\ 2}\right) \right]} = 1.0 \tag{46}$$

The maximum attainable Mach number for the primary flow when expanded to ambient pressure, M_{pO}, and the resultant exit Mach number of the ejector ramjet, M_{10}, can be found by these relations below [2, 6]:

$$M_{pO} = \sqrt{\frac{2}{\gamma_p - 1}\left[\left(\frac{P_{tp}}{P_O} \right)^{\frac{\gamma_p - 1}{\gamma_p}} - 1 \right]} \tag{47}$$

$$M_{10} = \sqrt{\frac{2}{\gamma_e - 1}\left[\left(\frac{P_{te}}{P_O}\right)^{\frac{\gamma_e - 1}{\gamma_e}} - 1\right]} \tag{48}$$

The total temperature of the primary and fully mixed flow, and the static temperature of that mixed flow are determined by these relations below:

$$T_{tp} = \frac{T_{tp}}{T_O} T_O \tag{49}$$

$$T_{te} = \frac{T_{te}}{T_O} T_O \tag{50}$$

$$T_e = \frac{T_e}{T_{tp}} T_{tp} \tag{51}$$

where $\frac{T_e}{T_{tp}} = \frac{2}{\gamma_e + 1}\frac{C_{pp}}{C_{pe}}\left(\frac{1 + \alpha\frac{C_{ps}}{C_{pp}}\frac{T_{ts}}{T_O}\frac{T_O}{T_{tp}}}{1 + \alpha}\right)$ [2].

According to Heiser & Pratt's ideal ejector ramjet model, the total temperature at the exhaust exit, T_{t10}, is approximately the same as the total temperature of the primary flow, T_{tp}, since the total temperature of the fully mixed flow is increased by the ramjet's main burner downstream of the shroud [2]. For such an ideal model that can be considered a very bold assumption. With that in mind, the static temperature at the exit of the ejector ramjet, T_{10}, and the static temperature of the primary flow at its maximum attainable Mach number, T_{pO}, can be found by these relations below:

$$T_{10} = \frac{T_{t10}}{1 + \frac{\gamma_e - 1}{2} M_{10}{}^2} \tag{52}$$

$$T_{pO} = \frac{T_{tp}}{1 + \frac{\gamma_p - 1}{2} M_{pO}{}^2} \tag{53}$$

From there, the velocity at the exhaust exit, V_{10}, the maximum attainable velocity of the primary flow, V_{pO}, and the flight velocity, V_O, can be obtained by the following relations below [2, 6]:

$$V_{10} = M_{10}\sqrt{\gamma_e R_e T_{10}} \tag{54}$$

$$V_{pO} = M_{pO}\sqrt{\gamma_p R_p T_{pO}} \tag{55}$$

$$V_O = M_O\sqrt{\gamma_s R_s T_O} \tag{56}$$

With that, the thrust augmentation ratio, ϕ_p, specific thrust, $\frac{F}{\dot{m}_p}$, and specific impulse, I_{sp}, can finally be calculated by the following relations below [2, 6]:

$$\phi_p = (1+\alpha)\frac{V_{10}}{V_{pO}} - \alpha\frac{V_O}{V_{pO}} \tag{57}$$

$$\frac{F}{\dot{m}_p} = \phi_p V_{pO} \tag{58}$$

$$I_{sp} = \frac{F/\dot{m}_p}{g_O} \tag{59}$$

where g_O is the acceleration due to gravity, which has a value of 9.81 m/s^2 for Earth. Those performance parameters above are calculated with the assumption of an ideal nozzle where exit pressure is perfectly expanded to ambient pressure, which is $\frac{P_{10}}{P_O} = 1$. This entire parametric cycle analysis of the ejector ramjet can be repeated for various flight conditions in terms of flight Mach number, ambient pressure, and ambient temperature.

2.3 Transatmospheric Performance Analysis for LEO

Another aspect in evaluating the maximum potential performance of the CRDWR is by calculating the minimum initial payload mass ratio, Γ, which is the ratio of the total initial mass of the launch vehicle over its payload mass. The smaller the value for Γ is, the more payload mass that could be lifted into orbit. In this study, that parameter will be determined for a two-stage launch vehicle to LEO in which the optimum value for Γ is found with a particular value of stage-separation Mach number. To do so, the first thing to determine is the reference trajectory through the atmosphere to LEO, which would be parameterized by altitude with corresponding velocity of the launch vehicle.

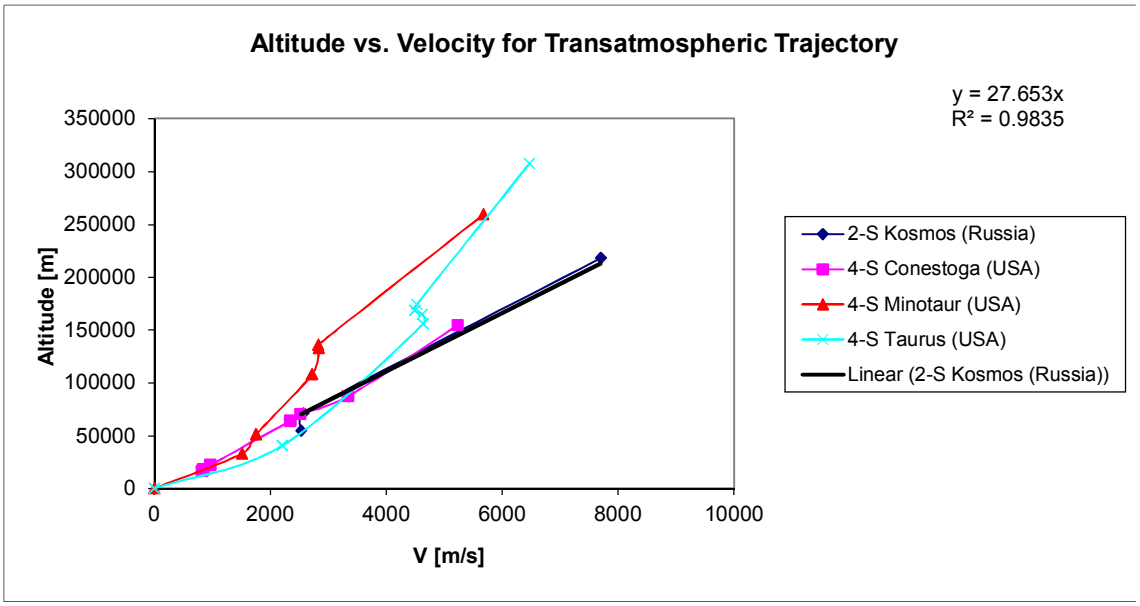

Figure 2.3 Plot of various launch trajectories in terms of altitude vs. velocity.

Figure 2.3 above provides a set of various trajectories of different rockets, of which the two-stage Kosmos rocket from Russia has the most appropriate trajectory for this study [7, 8]. Its launch trajectory is then mathematically quantified with a curve-fit trend line in the figure, which is represented by a black solid line with a corresponding equation of $h = (27.653)V_O$ for altitude in meters. For a particular flight velocity, an altitude is given by that equation, from

which the ambient pressure and temperature can be determined with the standard atmospheric tables. The corresponding flight Mach number at that velocity is then calculated by this relation below:

$$M_O = \frac{V_O}{\sqrt{\gamma_{air} R_{air} T_O}} \tag{60}$$

The flight Mach number, ambient pressure, and ambient temperature can then be fed as inputs into the parametric cycle analysis of the ejector-augmented CRDWR or CRDWR ejector ramjet for the first stage of the rocket. As for the CRDWR itself, only the ambient pressure from that set of parameters is needed for the parametric cycle analysis. For either the first stage or second stage of the launch vehicle, a parametric cycle analysis for the CRDWR with an attached spike nozzle was developed. Just like in the ejector ramjet cycle analysis, the spike nozzle is approximated as an ideal nozzle where the exhaust exit pressure is always perfectly expanded to ambient pressure. With the ambient pressure given along a certain trajectory, the first thing to calculate is the throat area of the CRDWR, which is given by this relation:

$$A_{throat} = \pi \frac{1}{4} d_c^{\,2} - \pi \frac{1}{4} \left(d_c - 2\Delta \right)^2 \tag{61}$$

Based on that, the total mass flow rate from the CRDWR is determined by this relation below:

$$\dot{m}_e = g_{throat} A_{throat} \tag{62}$$

where the specific flow rate at the throat, g_{throat}, is the same as g that was determined previously from Bykovskii's CRDWR model. The Mach number of the expanded exhaust flow of the CRDWR and its corresponding exit area are then calculated by these relations below [4]:

$$M_e = \sqrt{\left(\left[\frac{P_O}{P_{t,throat}} \right]^{\frac{-(\gamma_{throat}-1)}{\gamma_{throat}}} - 1 \right) \frac{2}{\gamma_{throat} - 1}} \tag{63}$$

$$A_e = A_{throat}\sqrt{\frac{1}{M_e^{\,2}}\left(\frac{2}{\gamma_{throat}+1}\left[1+\frac{\gamma_{throat}-1}{2}M_e^{\,2}\right]\right)^{\frac{\gamma_{throat}+1}{\gamma_{throat}-1}}} \tag{64}$$

where γ_{throat} and $P_{t,throat}$ are equal to the exit parameters of the CRDWR without the nozzle as determined previously from the parametric cycle analysis of Bykovskii's CRDWR model. The exit static temperature and exit velocity of the expanded flow from the CRDWR are then found by these relations below [4]:

$$T_e = \frac{T_{te}}{1+\frac{\gamma_{throat}-1}{2}M_e^{\,2}} \tag{65}$$

$$V_e = M_e\sqrt{\gamma_{throat}R_{throat}T_e} \tag{66}$$

From there, the thrust, specific thrust, and specific impulse of the CRDWR based on the flight conditions can finally be determined by these relations below (5):

$$F = \dot{m}_e V_e + A_e\left(P_e - P_O\right) \tag{67}$$

$$specific\_thrust = \frac{F}{\dot{m}_e} \tag{68}$$

$$I_{sp} = \frac{F}{\dot{m}_e g_O} \tag{69}$$

With the performance of the CRDWR repeatedly calculated by this parametric cycle analysis along the launch trajectory, the two-stage transatmospheric performance can then be carried out by first selecting the stage-separation Mach number, M_1. This corresponds to a separation flight velocity and altitude of the launch vehicle by the following relations:

$$V_1 = M_1\sqrt{\gamma_{air}R_{air}T_{O,avg}} \tag{70}$$

$$h_1 = \left(0.027653\right)V_1 \tag{71}$$

where $T_{O,avg}$ is the average ambient temperature for the entire atmosphere [2]. Based on how the specific impulse of the CRDWR or CRDWR ejector ramjet varies along the trajectory, the differential change in the mass of the launch vehicle can be determined by this relation [2]:

$$\frac{dm}{m} = -\left[\frac{d\left(\frac{V^2}{2}\right) + gdr}{g_O I_{sp} V\left(1 - \frac{D + D_e}{F}\right)}\right] \tag{72}$$

where r is the distance of the launch vehicle from the center of the Earth, and $1 - \frac{D + D_e}{F}$ is the installed thrust parameter. For LEO, the ratio $\frac{r}{r_O}$, where r_O is the radius of the Earth, is approximately close to 1 and therefore, the term gdr is omitted in equation (72) above. Since it is convenient to have that entire differential equation in terms of one variable on the right-hand side, $\frac{V^2}{2}$ is then set as variable b with the entire equation simplified into this relation below:

$$\frac{dm}{m} = \frac{-db}{g_O I_{sp}\sqrt{2b}\left(1 - \frac{D + D_e}{F}\right)} \tag{73}$$

where $1 - \frac{D + D_e}{F}$ has a constant average value for each rocket stage and I_{sp} is set as a function of variable V or $\sqrt{2b}$. Equation (73) is solved by using the classical 4th-order Runge-Kutta method in a MATLAB program based on these fundamental relations below [9]:

$$y' = f(x, y) \quad y(x_O) = y_O \tag{74}$$

$$k_1 = hf(x_n, y_n) \tag{75}$$

$$k_2 = hf\left(x_n + \frac{h}{2}, y_n + \frac{k_1}{2}\right) \tag{76}$$

$$k_3 = hf\left(x_n + \frac{h}{2}, y_n + \frac{k_2}{2}\right) \tag{77}$$

$$k_4 = hf\left(x_n + h, y_n + k_3\right) \tag{78}$$

$$y_{n+1} = y_n + \frac{k_1 + 2k_2 + 2k_3 + k_4}{6} \tag{79}$$

For this study, the variable y represents the mass m while variable *x* represents the velocity parameter b of the launch vehicle. As for the specific impulse function in equation (73), it is essentially the curve-fit trend line equation that approximates the variation of specific impulse of the propulsion system along the transatmospheric launch trajectory with respect to flight velocity. After solving equation (73) along the launch trajectory, an array of values for m with corresponding values for b is produced that is used to plot the variation of mass with respect to the velocity of the launch vehicle for the 1st stage. From that plot, a curve-fit trend line equation is created to approximate that variation. That equation is used to determine the final mass of stage 1 at the instant of separation, represented as $m_{1,final} = f\left(V_1\right)$, where V_1 is the flight velocity at stage separation. The fuel mass fraction of stage 1, Π_{f1}, and the initial payload mass ratio of stage 1, Γ_1, are then calculated by these relations below [2]:

$$\Pi_{f1} = 1 - \frac{m_{1,final}}{m_{i1}} \tag{80}$$

$$\Gamma_1 = \frac{1}{1 - \Pi_{e1} - \Pi_{f1}} \tag{81}$$

After stage separation, the initial mass of stage 2 is determined by this relation:

$$m_{2,initial} = m_{1,final} - \Pi_{e1} m_{i1} \tag{82}$$

At the end of stage 2 when the launch vehicle finally reaches LEO, the flight velocity and Mach number at that particular instant are calculated by these relations below:

$$V_{final} = \frac{h_{LEO}}{0.027653} \tag{83}$$

$$M_{final} = \frac{V_{final}}{\sqrt{\gamma_{air} R_{air} T_{O,avg}}} \tag{84}$$

where h_{LEO} is the altitude of LEO. To find the final mass of the launch vehicle at stage 2 after stage separation, equation (73) must be solved again for stage 2 where $m = m_{2,initial}$ and $b = \frac{V_1^2}{2}$ as the initial conditions. After solving, it again produces an array of values for m with corresponding values for b from stage separation all the way to LEO where $V = V_{final}$. They are then used to plot the variation of mass with respect to the velocity of the launch vehicle for the 2nd stage, from which a curve-fit trend line equation is again created. That equation is then used to determine the final mass of stage 2 when the launch vehicle reaches LEO, represented as $m_{2,final} = f\left(V_{final}\right)$. From there, the fuel mass fraction of stage 2, Π_{f2}, and the initial payload mass ratio of stage 2, Γ_2, can then be calculated by these relations below [2]:

$$\Pi_{f2} = 1 - \frac{m_{2,final}}{m_{2,initial}} \tag{85}$$

$$\Gamma_2 = \frac{1}{1 - \Pi_{e2} - \Pi_{f2}} \tag{86}$$

With the parameters for the 1st and 2nd stage calculated, the overall initial payload mass ratio, Γ, for the entire launch vehicle can finally be determined by this relation [2]:

$$\Gamma = \Gamma_1 \Gamma_2 \tag{87}$$

This entire two-stage transatmospheric performance analysis is then repeated for different stage-separation Mach numbers until the minimum value of Γ is obtained.

CHAPTER 3

RESULTS

With the analytical methodology developed to estimate the performance of the CRDWR in an ejector ramjet and a two-stage launch vehicle, calculations were carried out using a combination of Excel spreadsheets and MATLAB programs based on that methodology.

3.1 Specific Thrust and Specific Impulse Performance Results

In Excel, the calculations for the parametric cycle analysis of Bykovskii's CRDWR model is done in the spreadsheet shown in Table 3.1 below. As mentioned before, the pre-detonated pressure and temperature in the chamber is 1 atm and 300 K, using H_2-O_2 mixture.

Table 3.1 Parametric cycle analysis spreadsheet for Bykovskii's CRDWR model.

Initial conditions of the rocket chamber:					
P [atm]	T [K]				
1	300				
Total entalpy of the mixture (behind the detonation wave)					
input:				output:	
R-universal [J/(kmol-K)]	Molecular-weight [kg/kmol]			R-det [J/(kg-K)]	
8314.472	14.5			573.4	
gamma-det	R-det [J/(kg-K)]			Cp-det [J/(kg-K)]	
1.1288	573.4			5025.4	
Cp-det [J/(kg-K)]	T-det [K]	a-det [m/s]		h_O [J/kg]	h_O [kJ/kg]
5025.4	3675.81	1542.5		19661948.5	19661.9
input control variables:					
d_c [in]	corresponding d_c [m]	no. of transverse det. waves	h_1/l (optimum)		
98.4	2.5	2	0.175		
Bykovskii approach in calculating exit parameters for multiple TDW: (ref #1) (for constant area annular chamber - Model A)					
input:				output:	
n waves	d_c [m]			distance l between waves [m]	
2	2.5			3.93	
h_1/l	distance l [m]			h_1 [m]	
0.175	3.93			0.69	
h_1 [m]	k			h [m]	
0.69	0			0.69	
h [m]				Δ [m] (ref #1 eqn. 9)	
0.69				0.14	
h_1 [m]	Δ [m]	rho_2 [kg/m^3]	q_2 [m/s]	G_1 [kg/s]	
0.69	0.14	0.89689	1542.5	130.7	
G_1 [kg/s]	Δ [m]	distance l [m]		g (specific flow rate) [kg/(m^2-s)]	
130.7	0.14	3.93		242.1	
gamma-det	h_O [J/kg]			V_e [m/s]	
1.1288	19661948.5			1542.5	
g [kg/(m^2-s)]	V_e [m/s]	gamma-det		P_e [N/m^2]	
242.1	1542.5	1.1288		330829.5	
g [kg/(m^2-s)]	V_e [m/s]			rho-e [kg/m^3]	
242.1	1542.5			0.16	
P_e [N/m^2]	rho-e [kg/m^3]	V_e [m/s]	g [kg/(m^2-s)]	I_{sp} [m/s]	I_{sp} [sec]
330829.5	0.16	1542.5	242.1	2909.0	296.5
gamma-det	h_O [J/kg]			I_{sp} [m/s] (using 2nd eqn to verify)	I_{sp} [sec]
1.1288	19661948.5			2909.0	296.5

The exit parameters from the above spreadsheet are then fed into another spreadsheet that calculates the input parameters for the primary flow of the ejector ramjet, which is shown below in Table 3.2.

Table 3.2 Spreadsheet to get input parameters of the ejector ramjet's primary flow.

Parameters of primary flow for the Ejector-Augmented Rocket model: (the exit of the annular detonation rocket chamber)								
input:				output:				
V_e [m/s]	gamma-det	P_e [N/m^2]	rho-e [kg/m^3]	a_e [m/s]	M_e			
1542.5	1.1288	330829.5	0.16	1542.5	1			
gamma-det	M_e	R-det [J/(kg-K)]	a_e [m/s]	T_e [K]	T_{te} [K]			
1.1288	1	573.4	1542.5	3675.8	3912.5			
gamma-det	M_e	P_e [N/m^2]		P_{te} [N/m^2]				
1.1288	1	330829.5		571676.8		**Corresponding ambient freestream conditions:**		
P_O [N/m^2]	T_O [K]	P_{te} [N/m^2]	T_{te} [K]	**P_{tp}/P_O**	**T_{tp}/T_O**	M_O	P_O [N/m^2]	T_O [K]
936.9	222	571676.8	3912.5	**610.2**	**17.6**	3.68	936.93	222
gamma-det	R-det [J/(kg-K)]			**gamma-p**	**R_p [J/(kg-K)]**			
1.1288	573.4			**1.1288**	**573.4**			

The spreadsheet for calculating the input parameters for the secondary flow of the ejector ramjet is shown in Table 3.3 below.

Table 3.3 Spreadsheet for input parameters of the secondary flow.

Parameters of secondary flow:				
input:			output:	
gamma-air			gamma-s	
1.4			1.4	
gamma-s	M_O		T_{ts}/T_O	P_{tO}/P_O
1.4	3.68		3.71	98.64
$\pi_{d,max}$	η_r	P_{tO}/P_O	π_d	P_{ts}/P_O
0.96	0.72	98.64	0.69	67.78
R_{air} [J/(kg-K)]			R_s [J/(kg-K)]	
287			287	

The spreadsheet that contains other input parameters for the ejector ramjet, including the parameter for iteration, is shown in Table 3.4 below.

Table 3.4 Spreadsheet for other input parameters.

Iterative parameter:	
P_i/P_O:	61.72
Other input parameter:	
A/A_p *:	12

The parameters from Tables 3.2 to 3.4 are then fed into the parametric cycle analysis spreadsheet of the ejector ramjet or ejector-augmented rocket as shown below in Table 3.5.

Table 3.5 Parametric cycle analysis spreadsheet for the ejector ramjet.

Ejector-Augmented Rocket parametric cycle analysis:														
input:													output:	
gamma-p	P_{tp}/P_O	P_i/P_O:											Mpi	
1.1288	610.16	61.72											2.15	
gamma-s	P_{ts}/P_O	P_i/P_O:											M_{si}	
1.4	67.78	61.72											0.37	
M_{Pi}	gamma-p												A_{pi}/A_p^*	
2.15	1.1288												2.40	
A_{pi}/A_p^*	A/A_p^*:												A_{pi}/A	
2.40	12												0.20	
A_{pi}/A:													A_{si}/A	
0.20													0.80	
P_{ts}/P_O	P_{tp}/P_O	A_{si}/A	A_{pi}/A	M_{si}	M_{Pi}	T_{tp}/T_O	T_{ts}/T_O	gamma-p	gamma-s	R_p [J/(kg-K)]	R_s [J/(kg-K)]		α (bypass ratio)	
67.78	610.16	0.80	0.20	0.37	2.15	17.62	3.71	1.1288	1.4	573.41	287		2.08	
gamma-p	gamma-s	R_p [J/(kg-K)]	R_s [J/(kg-K)]										C_{pp} [J/(kg-K)]	C_{ps} [J/(kg-K)]
1.1288	1.4	573.41	287										5025.37	1004.50
α	C_{pp} [J/(kg-K)]	C_{ps} [J/(kg-K)]											C_{pe} [J/(kg-K)]	
2.08	5025.37	1004.5											2309.73	
R_p [J/(kg-K)]	R_s [J/(kg-K)]	α											R_e [J/(kg-K)]	
573.41	287	2.08											379.97	
C_{pe} [J/(kg-K)]	R_e [J/(kg-K)]												gamma-e	
2309.73	379.97												1.20	
α	C_{pp} [J/(kg-K)]	C_{pe} [J/(kg-K)]	C_{ps} [J/(kg-K)]	T_{tp}/T_O	T_{ts}/T_O								T_{te}/T_O	
2.08	5025.37	2309.73	1004.5	17.62	3.71								13.54	
gamma-e													P_e/P_{te}	
1.20													0.57	
gamma-e	gamma-p	R_s [J/(kg-K)]	R_p [J/(kg-K)]	M_{Pi}	P_{tp}/P_O	T_{tp}/T_O	A_{pi}/A	T_{te}/T_O:	α				P_{te}/P_O	
1.20	1.1288	379.97	573.41	2.15	610.16	17.62	0.20	13.54	2.08				109.41	
P_e/P_{te}	P_{te}/P_O:												P_e/P_O	
0.57	109.41												61.82	
P_e/P_O	P_O [N/m^2]	P_{te}/P_O											P_e [N/m^2]	P_{te} [N/m^2]
61.82	936.93	109.41											57924.87	102507.90
numerator:	$(P_e/P_O)*(1+\gamma_e)$		denominator	$(P_i/P_O)*[(A_{pi}/A)*(1+\gamma_p*M_{pi}\wedge 2)+(A_{si}/A)*(1+\gamma_s*M_{si}\wedge 2)]$									ratio: (iterative procedure)	
	135.82		135.85										1.00	
2/(gamma_e+1)	C_{pp}/C_{pe}	C_{ps}/C_{pp}	T_{ts}/T_O	T_O/T_{tp}	α								T_e/T_{tp}	
0.91	2.18	0.20	3.71	0.057	2.08								0.70	
gamma-p	P_{tp}/P_O	gamma-e	P_{te}/P_O:										M_{pO}	M_{10}
1.1288	610.16	1.20	109.41										4.09	3.44
T_{te}/T_O	T_{tp}/T_O	T_O [K]											T_{te} [K]	T_{tp} [K]
13.54	17.62	222											3005.44	3912.54
T_e/T_{tp}	T_{tp} [K]												T_e [K]	
0.70	3912.54												2736.07	
T_{tp} [K]													T_{t10} [K] (increased by downstream burner)	
3912.54													3912.54	
T_{t10} [K]	T_{tp} [K]	M_{10}	M_{pO}	gamma-e	gamma-p								T_{10} [K]	T_{pO} [K]
3912.54	3912.54	3.44	4.09	1.20	1.1288								1807.23	1882.04
M_O	gamma-s	R_s [J/(kg-K)]	T_O [K]										V_O [m/s]	
3.68	1.4	287	222										1100.00	
M_{pO}	gamma-p	R_p [J/(kg-K)]	T_{pO} [K]	M_{10}	gamma-e	R_e [J/(kg-K)]	T_{10} [K]						V_{10} [m/s]	V_{pO} [m/s]
4.09	1.1288	573.41	1882.04	3.44	1.20	379.97	1807.23						3118.55	4517.52
α	V_{10} [m/s]	V_{pO} [m/s]	V_O [m/s]										φ_p (thrust augmentation ratio)	
2.08	3118.55	4517.52	1100										**1.62**	
φ_p	V_{pO} [m/s]												F/m_p-dot [(N*s)/kg]	
1.62	4517.52												**7318.32**	
F/m_p-dot [N/(kg/s)]	g_O [m/s^2]												I_{sp} [sec]	
7318.32	9.81												**746.01**	

From the above spreadsheet in Table 3.5, the specific thrust and specific impulse of the ejector-augmented CRDWR is finally calculated. As for the CRDWR with an attached spike nozzle, a spreadsheet to calculate its specific thrust and specific impulse is shown in Table 3.6 below.

Table 3.6 Parametric cycle analysis spreadsheet for the CRDWR with a nozzle.

input control variable:						
P_{amb} or P_O [N/m^2]						
101325						
Sizing of Cylindrical Annular Chamber:						
input:		output:				
d_c [m]	Δ [m]	A_{throat} [m^2] (at the exhaust end of chamber)				
2.5	0.14	1.02				
Continuous Detonation Annular Rocket Chamber (Model A with nozzle expansion) parametric cycle analysis:						
input:					output:	
P_O [N/m^2]	$P_{t,throat}$ [N/m^2]	gamma-throat	A_{throat} [m^2]		M_e (where P_e=P_O)	Corresponding A_e [m^2]
101325	571676.8	1.1288	1.02		1.84	1.69
g_{throat} [kg/(m^2-s)]	A_{throat} [m^2]				m_e_dot [kg/s]	
242.1	1.02				247.0	
T_{te} [K]	M_e	gamma-throat	R_{throat} [J/(kg-K)]		T_e [K]	V_e [m/s]
3912.5	1.84	1.1288	573.4		3211.6	2654.3
m_e_dot [kg/s]	V_e [m/s]	A_e [m^2]	P_e [N/m^2]	P_O [N/m^2]	F [N]	F [kN]
247.0	2654.3	1.69	101325	101325	655556.9	655.6
F [N]	m_e_dot [kg/s]	g_O [m/s^2]			I_{sp} [sec]	F/m_e-dot [N/(kg/s)]
655556.9	247.0	9.81			270.6	2654.3

With those spreadsheets above, the performance calculations were carried out and tabulated for the constant q_O trajectory for both the CRDWR and the CRDWR ejector ramjet (ejector-augmented CRDWR) as shown in Tables 3.7 and 3.8 below.

Table 3.7 Recorded performance data of CRDWR with nozzle for constant q_O trajectory.

Constant q trajectory of 47,880 N/m^2 (1000 lbf/ft^2): (for const annular chamber w Expansion Nozzle, ideal case where $P_e = P_{amb}$)							
M_O (no effect on rocket)	altitude [m]	gamma	amb. pressure [N/m^2]	amb. Temperature [K]	q [N/m^2]	F/m_e-dot [N/(kg/s)]	Isp [sec]
0.2	0	1.4	101325.0	288.2	2837.1	2654.3	270.6
0.9	1500	1.4	84555.7	278.4	47943.1	2775.7	283.0
1.053	4000	1.4	61656.3	262.2	47855.5	2970.5	302.8
1.204	6000	1.4	47217.5	249.2	47913.0	3120.7	318.1
1.49	9000	1.4	30802.8	229.7	47869.7	3338.6	340.3
2.03	13000	1.4	16576.8	216.7	47817.8	3615.1	368.5
2.78	17000	1.4	8849.7	216.7	47876.0	3857.9	393.3
3.8	21000	1.4	4728.8	217.6	47799.1	4070.7	415.0
4.44	23000	1.4	3467.3	219.6	47847.6	4166.8	424.7
4.8	24000	1.4	2971.9	220.6	47930.2	4212.5	429.4
5.18	25000	1.4	2549.3	221.6	47883.4	4256.7	433.9
6.03	27000	1.4	1879.6	223.6	47840.2	4341.0	442.5
7.01	29000	1.4	1390.2	225.5	47819.5	4420.1	450.6
8.23	31000	1.4	1008.2	227.7	47803.3	4499.9	458.7

Table 3.8 Recorded performance data of CRDWR ejector ramjet for constant q_O trajectory.

Constant q trajectory of 47,880 N/m^2 (1000 lbf/ft^2):									
M_O	altitude [m]	gamma	amb. pressure [N/m^2]	amb. Temperature [K]	q [N/m^2]	thrust augmentation ratio	F/m_p-dot [N/(kg/s)]	Isp [sec]	α (bypass ratio)
0.2	0	1.4	101325.0	288.2	2837.1	1.16	3070.9	313.0	3.35
0.9	1500	1.4	84555.7	278.4	47943.1	2.01	5592.1	570.0	4.84
1.053	4000	1.4	61656.3	262.2	47855.5	1.96	5836.7	595.0	4.09
1.204	6000	1.4	47217.5	249.2	47913.0	1.96	6101.1	621.9	3.71
1.49	9000	1.4	30802.8	229.7	47869.7	2.02	6749.5	688.0	3.49
2.03	13000	1.4	16576.8	216.7	47817.8	2.38	8609.6	877.6	4.10
2.78	17000	1.4	8849.7	216.7	47876.0	3.42	13210.3	1346.6	6.90
3.8	21000	1.4	4728.8	217.6	47799.1	5.88	23928.9	2439.2	15.36
4.14	22000	1.4	3999.8	218.7	47988.4	6.81	28065.9	2860.9	19.38
4.44	23000	1.4	3467.3	219.6	47847.6	7.50	31233.6	3183.8	22.99
4.8	24000	1.4	2971.9	220.6	47930.2	8.17	34425.3	3509.2	27.48
5	24558.22	1.4	2736.0	221.1	47880.0	8.38	35515.4	3620.3	29.70
5.18	25000	1.4	2549.3	221.6	47883.4	8.50	36186.2	3688.7	31.61
6.03	27000	1.4	1879.6	223.6	47840.2	8.13	35277.9	3596.1	39.01
7.01	29000	1.4	1390.2	225.5	47819.5	6.38	28222.0	2876.9	45.31
8.23	31000	1.4	1008.2	227.7	47803.3	no solution	no solution	no solution	no solution

For the regular H_2-O_2 rocket counterpart in the ejector ramjet and its pure rocket mode, the following input spreadsheets were used as shown below in Tables 3.9 and 3.10, using the same total pressure of the chamber like in the CRDWR.

Table 3.9 Input spreadsheet for parametric cycle analysis of regular H_2-O_2 rocket ejector ramjet.

ambient freestream conditions:									
M_O	P_O [N/m^2]	T_O [K]					**From CEA Rocket code:**		
5.36	111.5	222					T_{tp} [K]	P_{tp} [N/m^2]	
							3309.47	571676.78	
Parameters of secondary flow:							**Parameters of primary flow:**			
input:			output:				P_{tp}/P_O	T_{tp}/T_O	gamma-p	R_p [J/(kg-K)]
gamma-air			gamma-s				5128.57	14.91	1.1193	547.00
1.4			1.4							
gamma-s	M_O		T_{ts}/T_O	P_{tO}/P_O			**Iterative parameter:**			
1.4	5.36		6.74	794.87			P_i/P_O:	251		
$\pi_{d,max}$	η_r	P_{tO}/P_O	π_d	P_{ts}/P_O						
0.96	0.45	794.87	0.44	347.11			**Other input parameter:**			
R_{air} [J/(kg-K)]			R_s [J/(kg-K)]				A/A_p*:	12		
287			287							

Table 3.10 Input spreadsheet for parametric cycle analysis of regular H_2-O_2 rocket with a nozzle.

input control variable:
P_{amb} or P_O [N/m^2]
5.85648E-10

Sizing of Exhaust Cylindrical Annular Chamber for Rocket:		
input:		output:
d_c [m]	Δ [m]	A_{throat} [m^2]
2.5	0.14	1.02

CEA: H2-O2 82.9-psi Rocket				
P_t [N/m^2]	gamma	R [J/(kg-K)]	P_{throat} [N/m^2]	T_t [K]
571676.8	1.1193	547.0	332390	3309.5

With that, the performance calculations were again carried out and recorded for the constant q_O trajectory for both the regular H_2-O_2 rocket and the regular H_2-O_2 rocket ejector ramjet. The performance comparison was then made between the CRDWR and its regular

H_2-O_2 rocket counterpart in terms of specific thrust and specific impulse with respect to flight Mach number for the constant q_O trajectory as shown below in Figures 3.1 to 3.4.

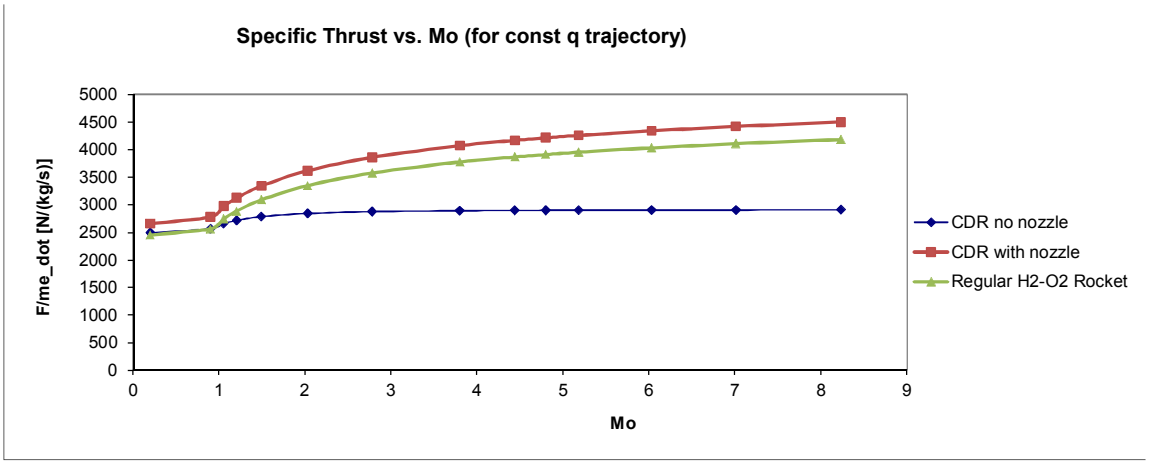

Figure 3.1 Specific thrust comparison between CRDWR and its regular H_2-O_2 rocket counterpart.

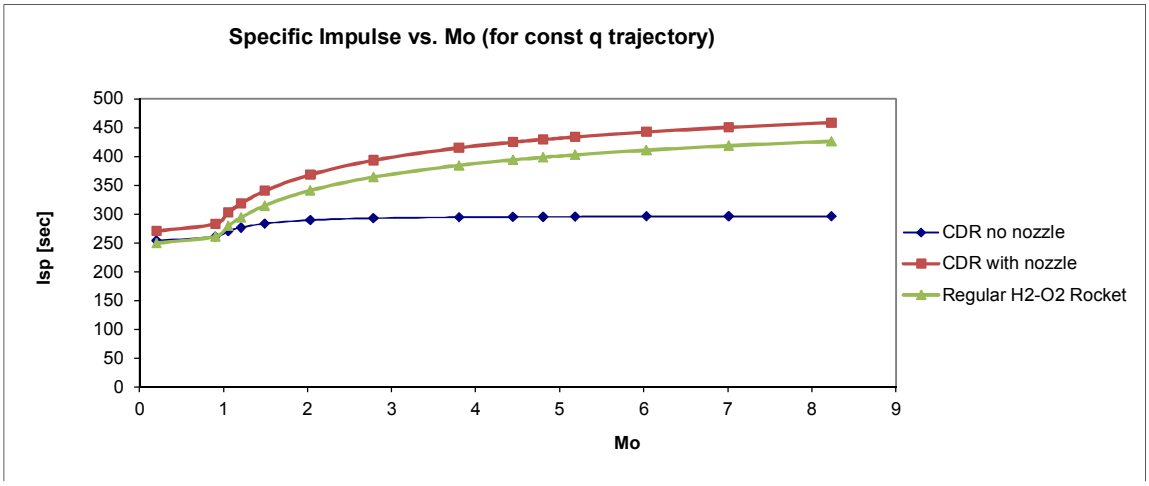

Figure 3.2 Specific impulse comparison between CRDWR and its regular H_2-O_2 rocket counterpart.

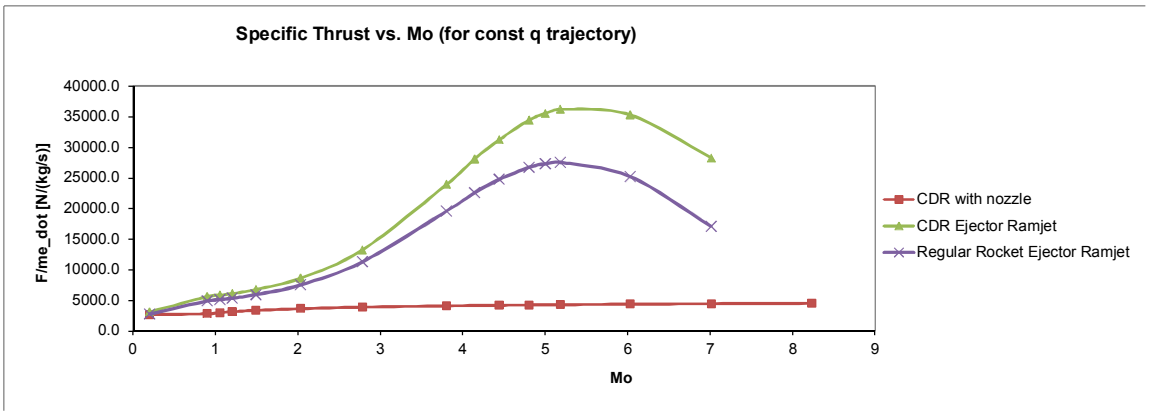

Figure 3.3 Specific thrust comparison between CRDWR ejector ramjet and the regular H_2-O_2 rocket ejector ramjet.

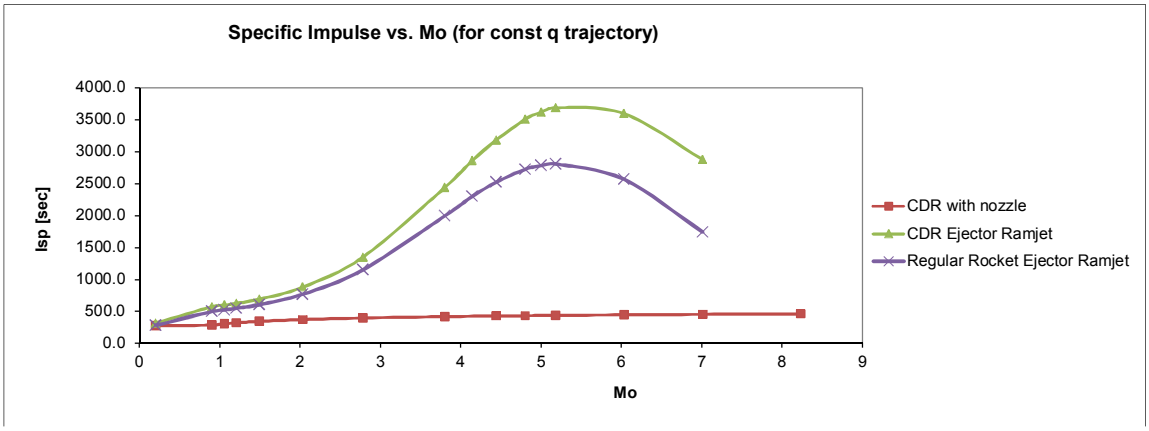

Figure 3.4 Specific impulse comparison between CRDWR ejector ramjet and the regular H_2-O_2 rocket ejector ramjet.

The specific thrust and specific impulse performance calculations were also carried out for the transatmospheric launch or vertical launch trajectory for both the CRDWR and the CRDWR ejector ramjet as recorded in Tables 3.11 and 3.12 below.

Table 3.11 Recorded performance data of CRDWR with nozzle for transatmospheric launch trajectory.

Vertical Launch Trajectory for CDR:								
V_O (no effect on rocket) [m/s]	altitude [m]	altitude [km]	gamma	amb. pressure [N/m^2]	amb. Temperature [K]	M_O (no effect on rocket)	F/m_e-dot [N/(kg/s)]	Isp [sec]
0	0	0.00	1.4	101325.0	222	0.00	2654.3	270.6
700	19357.1	19.36	1.4	5144.5	222	2.34	4043.6	412.2
1400	38714.2	38.71	1.4	261.2	222	4.69	4793.1	488.6
2100	58071.3	58.07	1.4	13.26	222	7.03	5261.8	536.4
2800	77428.4	77.43	1.4	0.67	222	9.38	5571.5	567.9
3500	96785.5	96.79	1.4	0.0342	222	11.72	5781.8	589.4
4200	116142.6	116.14	1.4	0.001735766	222	14.06	5926.9	604.2
4900	135499.7	135.50	1.4	8.81293E-05	222	16.41	6028.1	614.5
5600	154856.8	154.86	1.4	4.47455E-06	222	18.75	6099.1	621.7
6300	174213.9	174.21	1.4	2.27184E-07	222	21.09	6149.1	626.8
7000	193571	193.57	1.4	1.15347E-08	222	23.44	6184.5	630.4
7700	212928.1	212.93	1.4	5.85648E-10	222	25.78	6209.5	633.0

Table 3.12 Recorded performance data of CRDWR ejector ramjet for transatmospheric launch trajectory.

Vertical Launch Trajectory for CDR Ejector Ramjet:									
V_O [m/s]	altitude [m]	altitude [km]	gamma	amb. pressure [N/m^2]	amb. Temperature [K]	M_O	thrust augmentation ratio	F/m_e-dot [N/(kg/s)]	Isp [sec]
0	0	0.00	1.4	101325.0	222	0.00	1.17	3108.8	316.9
400	11061.2	11.06	1.4	18453.4	222	1.34	1.40	5007.8	510.5
700	19357.1	19.36	1.4	5144.5	222	2.34	1.60	6462.6	658.8
1100	30418.3	30.42	1.4	936.9	222	3.68	1.62	7318.3	746.0
1400	38714.2	38.71	1.4	261.2	222	4.69	1.45	6968.7	710.4
1500	41479.5	41.48	1.4	170.6	222	5.02	1.39	6789.2	692.1
1600	44244.8	44.24	1.4	111.5	222	5.36	no solution	no solution	no solution
2100	58071.3	58.07	1.4	13.26	222	7.03	no solution	no solution	no solution
2800	77428.4	77.43	1.4	0.6733	222	9.38	no solution	no solution	no solution
3500	96785.5	96.79	1.4	0.0342	222	11.72	no solution	no solution	no solution
4200	116142.6	116.14	1.4	0.001735766	222	14.06	no solution	no solution	no solution
4900	135499.7	135.50	1.4	8.81293E-05	222	16.41	no solution	no solution	no solution
5600	154856.8	154.86	1.4	4.47455E-06	222	18.75	no solution	no solution	no solution
6300	174213.9	174.21	1.4	2.27184E-07	222	21.09	no solution	no solution	no solution
7000	193571	193.57	1.4	1.15347E-08	222	23.44	no solution	no solution	no solution
7700	212928.1	212.93	1.4	5.85648E-10	222	25.78	no solution	no solution	no solution

With that, the performance comparison was again made between the CRDWR and its regular H_2-O_2 rocket counterpart in terms of specific thrust and specific impulse for the transatmospheric launch trajectory as shown below in Figures 3.5 and 3.6.

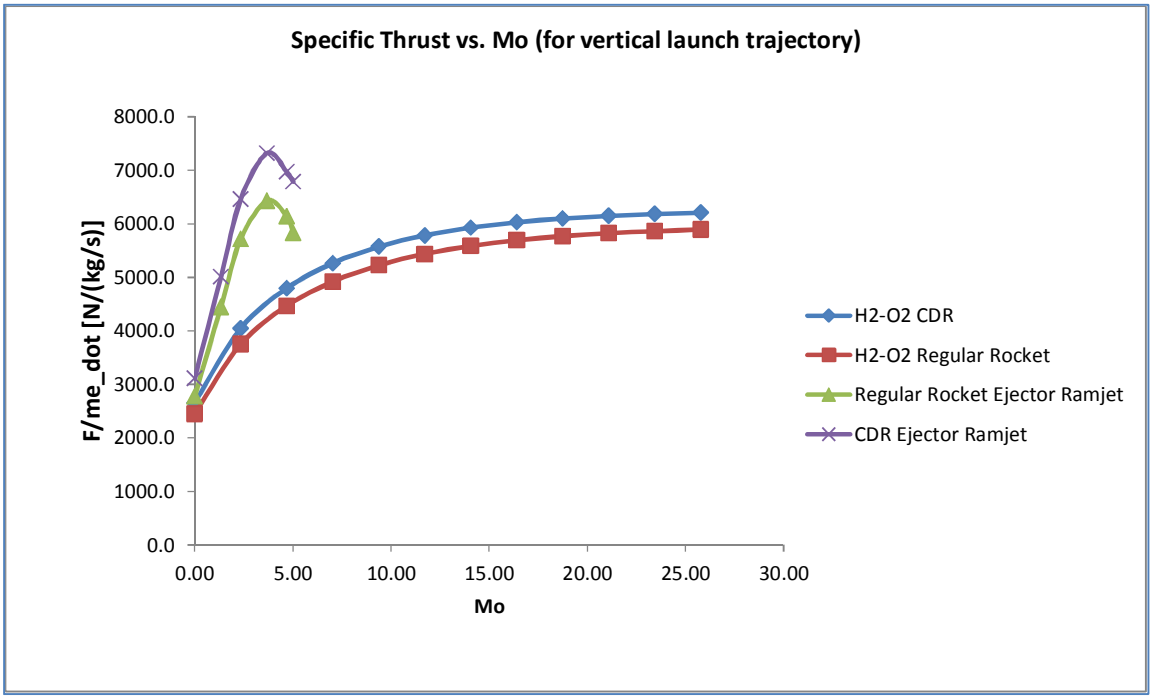

Figure 3.5 Specific thrust comparison between all four engines in transatmospheric launch trajectory.

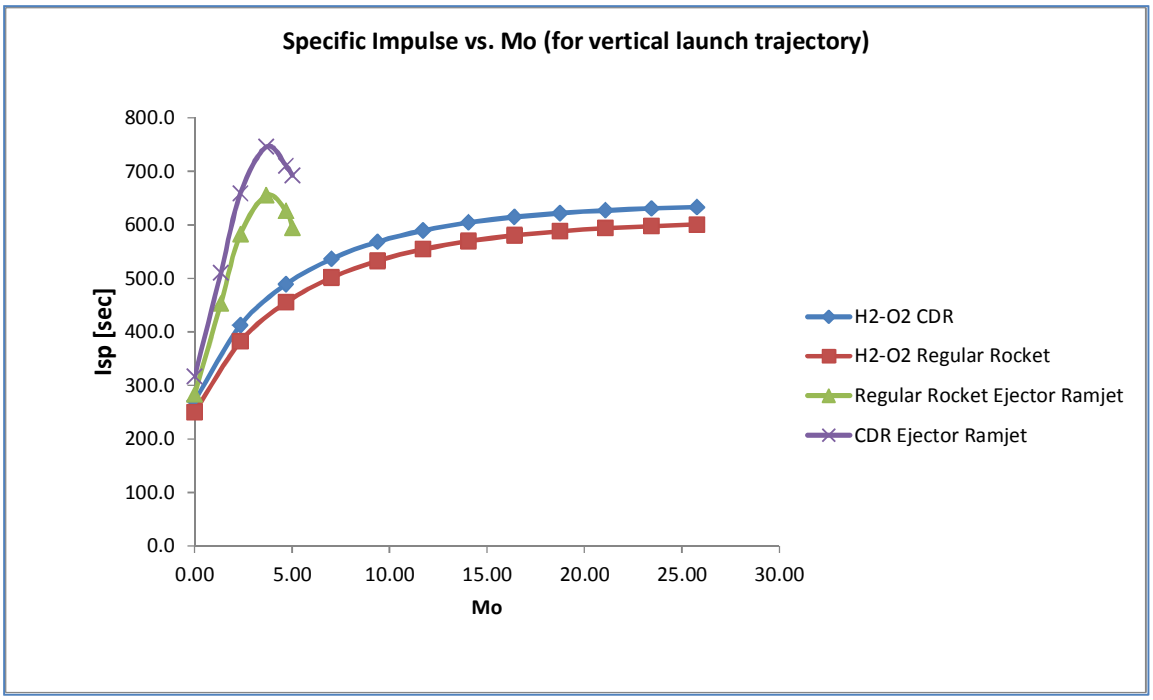

Figure 3.6 Specific impulse comparison between all four engines in transatmospheric launch trajectory.

From observing Figures 3.1 to 3.6, the CRDWR has exceeded the specific thrust and specific impulse performance of its regular H_2-O_2 rocket counterpart in both the pure rocket mode and the ejector ramjet mode while using identical values of total pressure in the rocket chamber. This is due to the fact that the detonation process in the CRDWR burns the propellant mixture more intensely with higher total temperature from the combustion than its regular H_2-O_2 rocket counterpart, thus leading to higher exhaust exit velocity from the engine.

3.2 Two-Stage Transatmospheric Performance Results

In Excel, calculations were also made for the transatmospheric performance of the two-stage launch vehicle with the CRDWR for both the 1st and 2nd stage by using the spreadsheet shown in Table 3.13 below.

Table 3.13 Performance analysis spreadsheet for a 2-stage CRDWR launch vehicle.

input control variable:							
π_{e1}	π_{e2}						
0.2	0.1						
2-Stage CDR:							
Input:					output:		
Stage Separation Mach number, M_1 (choose a value)					corresponding V_1 [m/s]	Corresponding h [km] (altitude)	
1.5					448.0	12.39	
V_1 [m/s] (at separation)			(using curve fit eqn. from MATLAB)		$m_{1,final}$ [kg]		
448.0					84519.7		
$m_{1,final}$ [kg]	m_{i1} [kg]				π_{f1}		
84519.7	100000				0.15		
π_{e1}	π_{f1}				Γ_1		
0.2	0.15				1.55		
π_{e1}	$m_{1,final}$ [kg]	m_{i1} [kg]			$m_{2,initial}$ [kg]		
0.2	84519.7	100000			64519.7		
final altitude [km]					V_{final} [m/s]	M_{final}	
200					7232.5	24.22	
V_{final} [m/s]			(using curve fit eqn. from MATLAB)		$m_{2,final}$ [kg]		
7232.5					17600		
$m_{2,final}$ [kg]	$m_{2,initial}$ [kg]				π_{f2}		
17600	64519.7				0.73		
π_{e2}	π_{f2}				Γ_2		
0.1	0.73				5.79		
Γ_1	Γ_2				Γ		
1.55	5.79				8.97		

For different stage-separation Mach numbers, the performance calculations for this launch vehicle are recorded below in Table 3.14.

Table 3.14 Recorded performance data of a 2-stage CRDWR launch vehicle.

separation Mach number	π_{f1}	Γ_1	π_{f2}	Γ_2	Γ
1.5	0.15	1.55	0.73	5.79	8.97
2	0.19	1.64	0.71	5.38	8.84
3	0.25	1.83	0.69	4.81	8.81
4	0.31	2.03	0.67	4.33	8.79
5	0.35	2.24	0.65	3.96	8.89
6	0.40	2.48	0.62	3.62	8.96
7	0.43	2.73	0.60	3.35	9.14
8	0.47	3.01	0.58	3.08	9.28
9	0.50	3.33	0.55	2.87	9.53
10	0.53	3.68	0.53	2.67	9.82

Similar calculations are also made for a launch vehicle where the CRDWR ejector ramjet is used for the 1st stage and the pure CRDWR for the 2nd stage using the transatmospheric performance analysis spreadsheet shown below in Table 3.15.

Table 3.15 Performance analysis spreadsheet for CRDWR-ER 1st stage, CRDWR 2nd stage launch vehicle.

CDR Ejector Ramjet 1st-Stage, CDR 2nd-Stage:							
Input:					output:		
Stage Separation Mach number, M_1 (choose a value)					corresponding V_1 [m/s]	Corresponding h [km] (altitude)	
5					1493.3	41.29	
V_1 [m/s] (at separation)			(using curve fit eqn. from MATLAB)		$m_{1,final}$ [kg]		
1493.3					73696.7		
$m_{1,final}$ [kg]	m_{i1} [kg]				π_{f1}		
73696.7	100000				0.26		
π_{e1}	π_{f1}				Γ_1		
0.2	0.26				1.86		
π_{e1}	$m_{1,final}$ [kg]	m_{i1} [kg]			$m_{2,initial}$ [kg]		
0.2	73696.7	100000			53696.7		
final altitude [km]					V_{final} [m/s]	M_{final}	
200					7232.5	24.22	
V_{final} [m/s]			(using curve fit eqn. from MATLAB)		$m_{2,final}$ [kg]		
7232.5					19000		
$m_{2,final}$ [kg]	$m_{2,initial}$ [kg]				π_{f2}		
19000	53696.7				0.65		
π_{e2}	π_{f2}				Γ_2		
0.1	0.65				3.94		
Γ_1	Γ_2				Γ		
1.86	3.94				7.34		

Although the above spreadsheet is similar to the one in Table 3.13, the curve-fit trend line equations from MATLAB (see Appendix A for the MATLAB programs used) that reflect the vehicle mass variations for each stage based on specific impulse variations are different for each spreadsheet. From the spreadsheet in Table 3.15, the performance calculations for this launch vehicle are recorded below in Table 3.16.

Table 3.16 Recorded performance data of CRDWR-ER 1st stage, CRDWR 2nd stage launch vehicle.

separation Mach number	π_{f1}	Γ_1	π_{f2}	Γ_2	Γ
2	0.15	1.54	0.71	5.38	8.27
3	0.19	1.64	0.69	4.79	7.87
4	0.23	1.75	0.67	4.35	7.59
5	0.26	1.86	0.65	3.94	7.34

With that, similar performance calculations were again carried out and recorded for the regular H_2-O_2 rocket counterpart. The performance comparison was then made between the 2-stage CRDWR, CRDWR-ER 1st stage & CRDWR 2nd stage, 2-stage regular H_2-O_2 rocket, and regular H_2-O_2 rocket-ER 1st stage & regular H_2-O_2 rocket 2nd stage launch vehicle in terms of overall initial payload mass ratio with respect to stage-separation Mach number for the transatmospheric trajectory to LEO as shown below in Figure 3.7.

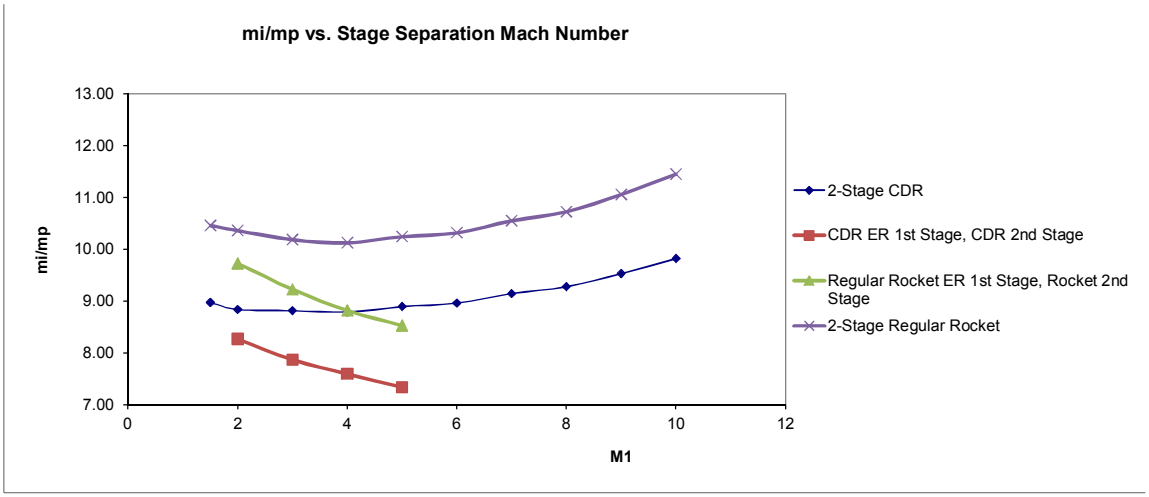

Figure 3.7 Comparison of initial payload mass ratio between all four launch vehicles in transatmospheric trajectory to LEO.

In Figure 3.7, the minimum value of Γ obtained is significantly lower for the CRDWR than for its regular H_2-O_2 rocket counterpart even though they have identical values of total pressure in the rocket chamber, which is promising. A higher specific impulse from the CRDWR will undoubtedly lead to lower initial payload mass ratio for the 2-stage launch vehicle. Based on Figure 3.7, a launch vehicle with the CRDWR ejector ramjet for the 1st stage and the CRDWR for the 2nd stage

would provide the best solution to reach LEO in which the stage separation occurs at around Mach 5.

3.3 CRDWR Performance at Higher Chamber Pressure

All these performance calculations above for the CRDWR were done where the pre-detonated chamber pressure is 1 atm. One wonders how much higher level of performance would the CRDWR obtain if the pre-detonated chamber pressure is increase to 12 atm, for example, while the pre-detonated chamber temperature is kept the same at 300 K? To find out, this input value is fed into the parametric cycle analysis spreadsheet of Bykovskii's CRDWR model as shown in Table 3.17 below.

Table 3.17 Parametric cycle analysis spreadsheet for Bykovskii's CRDWR model (12 atm - input).

Initial conditions of the rocket chamber:					
P [atm]	T [K]				
12	300				
Total entalpy of the mixture (behind the detonation wave)					
input:				output:	
R-universal [J/(kmol-K)]	Molecular-weight [kg/kmol]			R-det [J/(kg-K)]	
8314.472	15.113			550.2	
gamma-det	R-det [J/(kg-K)]			Cp-det [J/(kg-K)]	
1.1415	550.2			4438.2	
Cp-det [J/(kg-K)]	T-det [K]	a-det [m/s]		h_O [J/kg]	h_O [kJ/kg]
4438.2	4176.29	1619.5		19846455.3	19846.5
input control variables:					
d_c [in]	corresponding d_c [m]	no. of transverse det. waves	h_1/l (optimum)		
98.43	2.5	2	0.175		
Bykovskii approach in calculating exit parameters for multiple TDW: (ref #1) (for constant area annular chamber - Model A)					
input:				output:	
n waves	d_c [m]			distance l between waves [m]	
2	2.5			3.93	
h_1/l	distance l [m]			h_1 [m]	
0.175	3.93			0.69	
h_1 [m]	k			h [m]	
0.69	0			0.69	
h [m]				Δ [m] (ref #1 eqn. 9)	
0.69				0.14	
h_1 [m]	Δ [m]	rho_2 [kg/m^3]	q_2 [m/s]	G_1 [kg/s]	
0.69	0.14	10.73	1619.5	1641.4	
G_1 [kg/s]	Δ [m]	distance l [m]		g (specific flow rate) [kg/(m^2-s)]	
1641.4	0.14	3.926990817		3041.0	
gamma-det	h_O [J/kg]			V_e [m/s]	
1.1415	19846455.3			1619.5	
g [kg/(m^2-s)]	V_e [m/s]	gamma-det		P_e [N/m^2]	
3041.0	1619.5	1.1415		4314380.7	
g [kg/(m^2-s)]	V_e [m/s]			rho-e [kg/m^3]	
3041.0	1619.5			1.88	
P_e [N/m^2]	rho-e [kg/m^3]	V_e [m/s]	g [kg/(m^2-s)]	I_{sp} [m/s]	I_{sp} [sec]
4314380.7	1.88	1619.5	3041.0	3038.2	309.7
gamma-det	h_O [J/kg]			I_{sp} [m/s] (using 2nd eqn to verify)	I_{sp} [sec]
1.1415	19846455.3			3038.2	309.7

From Table 3.17, the specific impulse of the CRDWR turns out to be 309.7 sec as compared to 296.5 sec previously for 1 atm in pre-detonated chamber pressure. A slight 4.45 % increase in performance. With an attached ideal spike nozzle, its specific impulse was 412.9 sec at sea level and 642.2 sec at the vacuum as compared to 270.6 sec at sea level and 639.2 sec at the vacuum previously. This corresponds to a 52.6 % increase in performance at sea level, but only a 0.47 % increase in performance at the vacuum. This means that the CRDWR would already have close to maximum performance at a much smaller initial chamber pressure as compared to an already high chamber pressure of the regular rocket.

CHAPTER 4

CONCLUSIONS & RECOMMENDATIONS

Comparisons of performance between the CRDWR and the regular H_2-O_2 rocket as well as in their ejector-augmented forms were carried out in terms of specific thrust, specific impulse, and minimum values of initial payload mass ratio. All this was done while using the same total pressure in the rocket chamber. These comparisons were made along the constant q_O trajectory and the transatmospheric launch trajectory to LEO. As it turns out, both the CRDWR and the CRDWR ejector ramjet (ejector-augmented CRDWR) have higher specific thrust and specific impulse than their regular H_2-O_2 rocket counterparts. The use of the CRDWR in a 2-stage launch vehicle even allows for a lower value of initial payload mass ratio than its regular H_2-O_2 rocket counterpart. This would mean more payload mass that's able to reach orbit or a lighter overall takeoff weight of the 2-stage launch vehicle than ever before. For a moderately higher pre-detonated chamber pressure, the performance of the CRDWR increases significantly at low altitudes, but very marginally at high altitudes. This means that the CRDWR would have very high performance at a much lower initial chamber pressure than its regular rocket counterpart.

For future work, it is recommended that the validation of the parametric cycle analysis of Bykovskii's CRDWR model be carried out by comparing its performance results with the ones from the Endo-Fujiwara model of the CRDWR as well as experimental data produced by the Aerodynamics Research Center. As for the ideal rocket ejector model by Heiser & Pratt, one recommends changing the assumption about the increased total temperature by the ejector ramjet's main burner downstream of the fully mixed flow in order to produce a more realistic engine performance.

APPENDIX A

MATLAB PROGRAMS USED FOR TRANSATMOSPHERIC PERFORMANCE ANALYSIS

Transatmospheric_Isp_Variation_CDR.m file:

```
clear all; clc;
h=[0,19.3571,38.7142,58.0713,77.4284,96.7855,116.1426,135.4997,154.8568
,174.2139,193.571,212.9281];
Isp=[270.5697151,412.1905118,488.5889623,536.3751262,567.9415209,589.37
89525,604.1731964,614.4855983,621.7209344,626.8195807,630.4232601,632.9
755654];
plot(h,Isp,'*');
title('Specific Impulse vs. Altitude (for CDR)')
xlabel('Altitude [km]')
ylabel('Isp [sec]')
%from the graph: the curvefit trendline equation
Isp_funct_of_h=-(3.9015e-11)*h.^6+(2.9904e-8)*h.^5-(9.2905e-
6)*h.^4+0.0015318*h.^3-0.15089*h.^2+9.6752*h+270.75;
%-----------------------------------------------------------------------
--
V=[0,700,1400,2100,2800,3500,4200,4900,5600,6300,7000,7700];
figure, plot(V,Isp,'*');
title('Specific Impulse vs. Velocity (for CDR)')
xlabel('V [m/s]')
ylabel('Isp [sec]')
%from the graph: the curvefit trendline equation
Isp_funct_of_V=-(1.7446e-20)*V.^6+(4.8355e-16)*V.^5-(5.4326e-
12)*V.^4+(3.2391e-8)*V.^3-0.00011538*V.^2+0.26755*V+270.75;
%-----------------------------------------------------------------------
----
figure, plot(V,h,'*');
title('Altitude vs. Velocity (for CDR)')
xlabel('V [m/s]')
ylabel('Altitude [km]')
%from the graph: the curvefit trendline equation
h_funct_of_V=0.027653*V;
```

Transatmospheric_Isp_Variation_CDR_ejector_ramjet.m file:

```
clear all; clc;
h=[0,11.0612,19.3571,30.4183,38.7142,41.4795];
Isp=[316.8982114,510.4840372,658.7728709,746.0057514,710.3701675,692.06
79467];
plot(h,Isp,'*');
title('Specific Impulse vs. Altitude (for CDR ejector ramjet)')
xlabel('Altitude [km]')
ylabel('Isp [sec]')
%from the graph: the curvefit trendline equation
Isp_funct_of_h=(9.8627e-6)*h.^5-0.00063311*h.^4-
0.0043476*h.^3+0.45267*h.^2+13.735*h+316.9;
%-----------------------------------------------------------------------
--
V=[0,400,700,1100,1400,1500];
figure, plot(V,Isp,'*');
title('Specific Impulse vs. Velocity (for CDR ejector ramjet)')
xlabel('V [m/s]')
ylabel('Isp [sec]')
%from the graph: the curvefit trendline equation
```

```
Isp_funct_of_V=(1.5948e-13)*V.^5-(3.7021e-10)*V.^4-(9.1934e-
8)*V.^3+0.00034615*V.^2+0.37982*V+316.9;
%-------------------------------------------------------------------------
----
figure, plot(V,h,'*');
title('Altitude vs. Velocity (for CDR ejector ramjet)')
xlabel('V [m/s]')
ylabel('Altitude [km]')
%from the graph: the curvefit trendline equation
h_funct_of_V=0.027653*V;
```

RK4_CDR.m file:

```
function [m,b] = RK4_CDR(h,duration,x1,y1,ITP)
N=duration/h;
go=9.81;
f=@(x,y) (-y)/(go*(-(1.7446e-20)*sqrt(2*x)^6+(4.8355e-16)*sqrt(2*x)^5-
(5.4326e-12)*sqrt(2*x)^4+(3.2391e-8)*sqrt(2*x)^3-
0.00011538*sqrt(2*x)^2+0.26755*sqrt(2*x)+270.75)*sqrt(2*x)*ITP);
m(1) = y1;
for i = 1:N
k1=h*f(x1+(i-1)*h,m(i));
k2=h*f(x1+(i-1)*h+(h/2),m(i)+(k1/2));
k3=h*f(x1+(i-1)*h+(h/2),m(i)+(k2/2));
k4=h*f(x1+(i-1)*h+h,m(i)+k3);

m(i+1)=m(i)+(k1 + 2*k2 + 2*k3 + k4)/6;
b(i)=x1+(i-1)*h;
end
b(N+1)=b(N)+h;
end
```

RK4_CDR_ER.m file:

```
function [m,b] = RK4_CDR_ER(h,duration,x1,y1,ITP)
N=duration/h;
go=9.81;
f=@(x,y) (-y)/(go*((1.5948e-13)*sqrt(2*x)^5-(3.7021e-10)*sqrt(2*x)^4-
(9.1934e-
8)*sqrt(2*x)^3+0.00034615*sqrt(2*x)^2+0.37982*sqrt(2*x)+316.9)*sqrt(2*x
)*ITP);
m(1) = y1;
for i = 1:N
k1=h*f(x1+(i-1)*h,m(i));
k2=h*f(x1+(i-1)*h+(h/2),m(i)+(k1/2));
k3=h*f(x1+(i-1)*h+(h/2),m(i)+(k2/2));
k4=h*f(x1+(i-1)*h+h,m(i)+k3);

m(i+1)=m(i)+(k1 + 2*k2 + 2*k3 + k4)/6;
b(i)=x1+(i-1)*h;
end
b(N+1)=b(N)+h;
end
```

Transatmospheric_Performance_CDR.m file:

```
%for pure continuous detonation rocket for all 2-stages:
clear all; clc;
m1_initial=100e3; %<---initial mass of the entire rocket [kg]
%V_initial=sqrt(2); %<---in [m/s]
%b_initial=0.5*V_initial^2;
%ITP_1=0.9; %<---installed thrust parameter for Stage 1
%[m,b]=RK4_CDR(300,9.9e6,b_initial,m1_initial,ITP_1);
%V=sqrt(2*b);
%Isp=-(1.7446e-20)*V.^6+(4.8355e-16)*V.^5-(5.4326e-12)*V.^4+(3.2391e-
8)*V.^3-0.00011538*V.^2+0.26755*V+270.75;
%h=0.027653*V; %<---altitude [km]
%M=V/sqrt(1.4*287*222);
%figure, plot(V,m); title('Rocket Mass vs. Velocity (1st Stage)');
%xlabel('V [m/s]'); ylabel('m [kg]')
%from the graph: the curvefit trendline equation
%for m_i=100e3 kg:
%m_funct_of_V=-(5.4663e-21)*V.^7+(1.0549e-16)*V.^6-(8.5807e-
13)*V.^5+(3.8613e-9)*V.^4-(1.0759e-5)*V.^3+0.020869*V.^2-
39.434*V+98824;
%hold on, plot(V,m_funct_of_V);
%-------------------------------------------------------------------------
%-------------------------------------------------------------------------
%begin transatmospheric performance calculations:
%Let's choose a separation Mach number for Stage 1:
M=1.5; %<---separation Mach number
V=M*sqrt(1.4*287*222); %<---corresponding velocity at stage separation
m_at_separation=-(5.4663e-21)*V^7+(1.0549e-16)*V^6-(8.5807e-
13)*V^5+(3.8613e-9)*V^4-(1.0759e-5)*V^3+0.020869*V^2-39.434*V+98824;
pi_f1=1-m_at_separation/m1_initial;
%corresponding altitude [km]
h=0.027653*V;
%-------------------------------------------------------------------------
%for Stage 2:
pi_e1=0.2; %<---structural mass fraction of Stage 1
m2_initial=m_at_separation-pi_e1*m1_initial;
V2_initial=V; %<---velocity at stage separation
b2_initial=0.5*V2_initial^2;
ITP_2=0.95; %<---installed thrust parameter for Stage 2
[m2,b2]=RK4_CDR(900,2.7e7,b2_initial,m2_initial,ITP_2);
V2=sqrt(2*b2);
figure, plot(V2,m2); title('Rocket Mass vs. Velocity (2nd Stage)');
xlabel('V [m/s]'); ylabel('m [kg]');
V_final=200/0.027653;
%from the graph: the curvefit trendline equation
%(it changes with separation Mach number, so you need to update it)
%m2_final=-(3.3294e-24)*V_final^7+(9.6483e-20)*V_final^6-(1.5024e-
15)*V_final^5+(1.9703e-11)*V_final^4-(2.1142e-
7)*V_final^3+(0.0016731)*V_final^2-10.23*V_final+42656;
```

Transatmospheric_Performance_CDR_ejector_ramjet.m file:

```
%for CDR ejector ramjet 1st stage, CDR 2nd stage:
clear all; clc;
m1_initial=100e3; %<---initial mass of the entire rocket [kg]
%V_initial=sqrt(2); %<---in [m/s]
%b_initial=0.5*V_initial^2;
%ITP_1=0.9; %<---installed thrust parameter for Stage 1
%[m,b]=RK4_CDR_ER(300,3.6e6,b_initial,m1_initial,ITP_1);
%V=sqrt(2*b);
%Isp=(1.5948e-13)*V.^5-(3.7021e-10)*V.^4-(9.1934e-
8)*V.^3+0.00034615*V.^2+0.37982*V+316.9;
%h=0.027653*V; %<---altitude [km]
%M=V/sqrt(1.4*287*222);
%figure, plot(V,m); title('Rocket Mass vs. Velocity (1st Stage)');
%xlabel('V [m/s]'); ylabel('m [kg]')
%from the graph: the curvefit trendline equation
%for m_i=100e3 kg:
%m_funct_of_V=-(1.0867e-19)*V.^7+(3.3833e-16)*V.^6+(1.0431e-12)*V.^5-
(3.4459e-9)*V.^4-(3.6206e-6)*V.^3+0.01962*V.^2-33.164*V+98963;
%hold on, plot(V,m_funct_of_V);
%-------------------------------------------------------------------
%-------------------------------------------------------------------
%begin transatmospheric performance calculations:
%Let's choose a separation Mach number for Stage 1:
M=5; %<---separation Mach number
V=M*sqrt(1.4*287*222); %<---corresponding velocity at stage separation
m_at_separation=-(1.0867e-19)*V^7+(3.3833e-16)*V^6+(1.0431e-12)*V^5-
(3.4459e-9)*V^4-(3.6206e-6)*V^3+0.01962*V^2-33.164*V+98963;
pi_f1=1-m_at_separation/m1_initial;
%corresponding altitude [km]
h=0.027653*V;
%-------------------------------------------------------------------
%for Stage 2:
pi_e1=0.2; %<---structural mass fraction of Stage 1
m2_initial=m_at_separation-pi_e1*m1_initial;
V2_initial=V; %<---velocity at stage separation
b2_initial=0.5*V2_initial^2;
ITP_2=0.95; %<---installed thrust parameter for Stage 2
[m2,b2]=RK4_CDR(900,2.7e7,b2_initial,m2_initial,ITP_2);
V2=sqrt(2*b2);
figure, plot(V2,m2); title('Rocket Mass vs. Velocity (2nd Stage)');
xlabel('V [m/s]'); ylabel('m [kg]');
V_final=200/0.027653;
%from the graph: the curvefit trendline equation
%(it changes with separation Mach number, so you need to update it)
%m2_final=-(3.3294e-24)*V_final^7+(9.6483e-20)*V_final^6-(1.5024e-
15)*V_final^5+(1.9703e-11)*V_final^4-(2.1142e-
7)*V_final^3+(0.0016731)*V_final^2-10.23*V_final+42656;
```

REFERENCES

[1] Bykovskii, F. A., Zhdan, S. A., and Vedernikov, E. F., "Continuous Spin Detonations," Vol. 22, No. 6, AIAA, 2006.

[2] Heiser, W. H. and Pratt, D. T., "Hypersonic Airbreathing Propulsion,", AIAA Education Series, 1994.

[3] Gordon, S. and McBride, B. J., "Computer Program for Calculation of Complex Chemical Equilibrium Compositions and Applications," NASA RP 1311, 1994 (http://www.grc.nasa.gov/WWW/CEAWeb/)

[4] Anderson, J. D., "Modern Compressible Flow," 3rd ed., McGraw Hill, International Edition, 2004.

[5] Mattingly, J. D. and Ohain, H., "Elements of Propulsion: Gas Turbines and Rockets," AIAA Education Series, Reston, VA, 2006.

[6] Hekiri, H., Kim, J., Lu, F. K., and Wilson, D. R., "Analysis of an Ejector-Augmented Pulse Detonation Rocket," AIAA Paper 2008-0114, 2008.

[7] Isakowitz, S. J., "International Reference Guide to Space Launch Systems," 2nd ed., AIAA, Washington D.C., 1995.

[8] Isakowitz, S. J., Hopkins, J. B., and Hopkins, J. P., Jr., "International Reference Guide to Space Launch Systems," 4th ed., AIAA, Reston, VA, 2004.

[9] McCalla, T. R., "Introduction to Numerical Methods and FORTRAN Programming," John Wiley & Sons, Inc., NY, 1967.

BIOGRAPHICAL INFORMATION

Huan Cao was born in Dallas, Texas on November of 1985 by parents who came from Vietnam. As a second-generation Asian-American born of mixed Vietnamese/Chinese blood, Huan was raised in Dallas and attended an elementary school there. In 2000, he and his family moved to Keller, Texas where he then attended Keller High School. Later in 2004, Huan enrolled at the University of Texas at Arlington to pursue his bachelor's degree and soon after, his master's degree in aerospace engineering. Huan's specific field of interest is in high-speed combined-cycle propulsion that is appropriate for transatmospheric flight to LEO. Currently, he is planning on doing his Ph.D. program at UT Arlington, starting in Fall of 2011.